Visualised predictions of gap anisotropy to test new electron pairing scheme

Zheng, X. H., & Walmsley, D. G. (2017). Visualised predictions of gap anisotropy to test new electron pairing scheme. Physica C: Superconductivity and its Applications, 534, 19-28. https://doi.org/10.1016/j.physc.2016.12.007

Published in:
Physica C: Superconductivity and its Applications

Document Version:
Peer reviewed version

Queen's University Belfast - Research Portal:
Link to publication record in Queen's University Belfast Research Portal

Visualised predictions of gap anisotropy to test new electron pairing scheme

X. H. Zheng and D. G. Walmsley
*Department of Physics and Astronomy, Queen's University of Belfast, BT7 1NN, N. Ireland**
(Dated: December 20, 2016)

The rich and fertile but not yet adequately exploited ground of superconductor anisotropy is proposed as a test bed for a new empirical scheme of electron pairing. The scheme is directed to resolving a numerical and conceptual difficulty in the BCS theory. The original theoretical formulation of the anisotropy problem by Bennett is adopted and its outcomes extensively explored. Here the Bennett conclusion that in metallic superconductors phonon anisotropy is the principal source of gap anisotropy is accepted. Values of the energy gap are visualised globally in **k**-space with unprecedented detail and accuracy. Comparison is made between the anisotropy pattern from the new and the usual BCS pairing schemes. Differences are revealed for future experimental resolution.

PACS numbers: 71.15.Dx, 74.25.Kc, 31.10.+z

I. INTRODUCTION

Since a superconducting transition temperature (T_c) up to 203 K has been observed in the sulphur hydride system, with a definite isotope effect [1], the classic theory of Bardeen, Cooper and Schrieffer (BCS) [2] and its generalised version due to Eliashberg [3] have returned to centre stage [4]. Indeed it was the theoretical work of Li et al based on BCS-Eliashberg theory which first predicted that sulphur hydride under pressure has a high potential to be superconductive, possibly at temperatures up to 82K [5]. The BCS-Eliashberg theory is universally accepted as providing the best microscopic description of phonon-mediated superconductivity. However, over the years it has shown some uncomfortable signs of strain and received criticism [6]. A recent study by Durajski has refined the Eliashberg equations by taking into account the lowest order vertex correction [7, 8]. Our anticipation is that the BCS theory is fundamentally healthy and will deliver exceptionally good outcomes to meet the current demand when its specific difficulties have been identified and remedied.

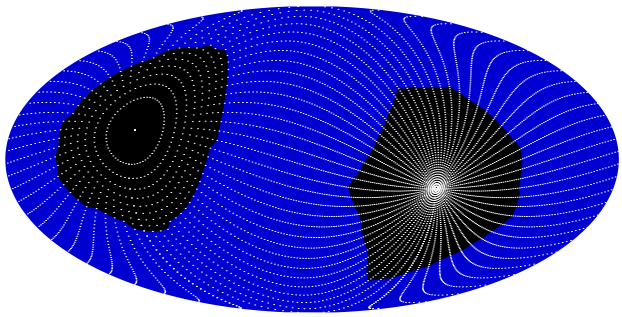

FIG. 1: Traces (white dots) of electron paths over the Fermi surface in lead as a result of normal and umklapp scattering. In each azimuthal direction the absolute value of the electron momentum, **k**, increases in equal steps; for geometrical reasons the dots appear to be denser around the initial state, $\mathbf{k}_0$, but more sparse towards the paired state $-\mathbf{k}_0$. The ranges of normal phonon scattering from $\mathbf{k}_0$ and $-\mathbf{k}_0$ are indicated as black areas.

The BCS theory has always suffered from a numerical difficulty: there is an inconsistency in outcome when the electron-phonon interaction assumed in the theory of electrical resistivity in the normal state is used in it. The literature shows that either superconductivity from the BCS theory is too strong when the calculated resistivity is reasonable or, conversely but equivalently, resistivity is too weak when superconductivity is reasonable: somehow the phonon contribution to superconductivity is excessive and needs to be curtailed [9, 10].

We have also identified a conceptual difficulty in the BCS theory [9, 10]. We have introduced an empirical scheme of electron pairing to overhaul the theory both conceptually and numerically [9–11]. It can be presented analytically as a survival rate, $S(\mathbf{q}) = 0$ or $1/2$, depending on whether or not scattered electron pairs fall into the black areas in FIG. 1, $\mathbf{q}$ being the momentum of the phonons scattering the electrons (see FIG. 2). Extensive tests demonstrate that the numerical difficulty of the BCS theory also is remedied to high accuracy when this consideration is taken into account [9–13].

We now seek further tests of this new empirical pairing scheme. To this end we recall the view of Joynt and Taillefer [14] that "the student of magnetism has the luxury of being able to consult neutron diffraction data from which the magnetic structure can be read off. In superconductivity, the order parameter sets up no measurable field and there is no experimental probe which couples directly to it. Precisely for the reason that experiments to determine the order parameter structure are so indirect, a very close connection between experiment and theory is essential." We propose to test the new pairing scheme on the rich and fertile but not yet adequately exploited grounds of superconducting energy gap anisotropy.

Our test will be based on the framework of Bennett [16]. It starts with the isotropic electron-phonon spec-

*Electronic address: dg.walmsley@qub.ac.uk

tral density $\alpha^2F(\nu)$ that leads to an isotropic energy gap, $\overline{\Delta}(\omega)$ (dirty limit). Bennett argues that a metallic superconductor is largely isotropic, so that he keeps $\overline{\Delta}(\omega)$ but replaces $\alpha^2F(\nu)$ with its anisotropic generalisation and thus finds superconductor anisotropy. Bennett evaluated his theory for lead with the realistic phonon data available to him. Both the initial and final electron states are placed on the Fermi surface exactly in accordance with the physics. Bennett considered both spherical and more realistic Fermi surfaces and compared the results. He concluded that phonon anisotropy is the principal source of gap anisotropy.

Following the Bennett approach carefully, we place both the initial and end states of the electrons exactly on a spherical Fermi surface. In addition we visualise gap anisotropy globally in **k**-space with unprecedented resolution and accuracy and make a detailed comparison between the outcomes from our empirical pairing scheme and the BCS scheme. Available experimental data appear to give marginal support to the new scheme but are inconclusive. We look forward to future better experimental scrutiny and pairing scheme resolution.

Our article is arranged as follows. In Sections II and III we outline briefly the Bennett theory of gap anisotropy. The experimental situation is reviewed in Section IV. In Sections V and VI we review an historical difficulty of the BCS theory and the new pairing scheme to resolve it. In Section VII we study lead with the new and also, for comparison, the conventional BCS pairing scheme. In VIII we comment on previous lead studies. In Sections IX, X and XI we study aluminium, niobium and tantalum also with both schemes. Brief conclusions are presented in Section XII.

II. BENNETT THEORY

Anderson [15] first highlighted the significance of the phenomenon of superconductor anisotropy in 1959. Bennett [16] then developed a formulation for anisotropic superconductivity in real metals. In it the following equations determine the anisotropic superconducting energy gap to a good approximation:

$$\Delta(\omega) = \frac{1}{Z(\omega)} \int_0^\infty d\omega' \, \Re \left[\frac{\overline{\Delta}(\omega')}{\sqrt{\omega'^2 - \overline{\Delta}(\omega')^2}} \right] K_\Delta(\omega, \omega')$$

$$Z(\omega) = 1 + \frac{1}{\omega} \int_0^\infty d\omega' \, \Re \left[\frac{\omega'}{\sqrt{\omega'^2 - \overline{\Delta}(\omega')^2}} \right] K_Z(\omega, \omega') \tag{1}$$

where, when $T = 0$,

$$K_\Delta(\omega, \omega') = \int_0^\infty d\nu \; \alpha^2F(\nu) \left[\frac{1}{\nu + \omega' - \omega - i0^+} + \frac{1}{\nu + \omega' + \omega + i0^+} - \mu^* \right]$$

$$K_Z(\omega, \omega') = \int_0^\infty d\nu \; \alpha^2F(\nu) \left[\frac{1}{\nu + \omega' - \omega - i0^+} - \frac{1}{\nu + \omega' + \omega + i0^+} \right] \tag{2}$$

μ^* being the Coulomb pseudopotential. Here $\Delta(\omega) = \Delta(\omega, \varphi, \theta)$, $\overline{\Delta}(\omega)$ its average over φ and θ (dirty limit) and $\alpha^2F(\nu) = \alpha^2F(\nu, \varphi, \theta)$, the anisotropic electron-phonon spectral density.

We can replace $\Delta(\omega)$ on the left hand side of Eq. (1) with $\overline{\Delta}(\omega)$, provided that we also replace $\alpha^2F(\nu)$ with its values averaged over φ and θ. Consequently Eqs. (1) and (2) become the familiar equations for the isotropic energy gap function, ready to be solved for $\overline{\Delta}(\nu)$. Afterwards, with $\alpha^2F(\nu) = \alpha^2F(\nu, \varphi, \theta)$ in Eq. (2) to manifest phonon anisotropy, we can readily find $\Delta(\omega) = \Delta(\omega, \varphi, \theta)$. This procedure is exact if we accept Eqs. (1) and (2) as a valid starting point. It is not an iterative procedure truncated in the first round: Bennett starts from a theory allowing no room for further iteration.

When solving Eq. (1) the workload rests mostly on estimating the strength of the electron-phonon interaction from first principles. For lead, niobium and tantalum we start from the following muffin-tin atomic pseudopotential:

$$V(r) = \delta V \cos\left(\frac{\pi r}{2r_1}\right), \quad \text{when } r < r_1 \tag{3}$$

otherwise $V(r) = 0$. With detailed phonon knowledge we can find from Eq. (3) both the electron-phonon superconducting spectral density, $\alpha^2F(\nu)$, and the electron-phonon transport density, $\alpha^2_{\rm tr}F(\nu)$, for electrical resistivity in the normal state, see [12] for details. The extent of phonon involvement can be appreciated from FIG. 1 where the end states are aligned along one half of a great circle from $\mathbf{k}_0$ to $-\mathbf{k}_0$ at 101 locations. Furthermore, we have 80 such half great circles crossing the initial electron state $\mathbf{k}_0$. We also have 210 values of $\mathbf{k}$ in an irreducible section of the Fermi surface, that is a spherical triangle with its vertices in the [100], [110] and [111] directions, so that in total we have to solve 1,696,800 sets of 3×3 eigen-equations for phonon frequencies. These are precalculated and stored in look-up tables for subsequent ready use; otherwise the task becomes insurmountable.

III. BENNETT CONCLUSION

In 1964 Geilikman and Kresin studied the effect of anisotropy on the properties of superconductors theoret-

ically within the framework of the Bogolyubov formalism [18]. They adopted a Debye phonon model, with an isotropic phonon distribution and without umklapp processes. Therefore their source of superconducting energy gap anisotropy was the band structure anisotropy acting through the matrix element of the electron-phonon interaction; it is entirely from the non-spherical shape of the Fermi surface. They evaluated gap anisotropy analytically with two types of model Fermi surfaces: closed (ellipsoid) and open (cylindrical).

In 1965 Bennett studied a similar ellipsoidal Fermi surface model within the BCS formalism. The phonons are assumed to be from a so-called modified Einstein model, in which the phonon frequency is largely fixed but perturbed by the projection of the phonon wave vector on the symmetry axis. Bennett found that the effect of the non-spherical Fermi surface on gap anisotropy, either from his own calculations or from [18], is much smaller than the phonon effect.

Bennett also studied superconductor anisotropy in lead within the framework of the BCS-Eliashberg-Nambu formalism [16]. The phonons are from experimental measurement by neutron scattering along high-symmetry directions. Phonons along other directions are from interpolation with Kubic harmonics. The initial and end electron states are placed on a spherical Fermi surface, with 26 values of the angular coordinates of the end states chosen randomly, compared with the numerous end states shown as white dots in FIG. 1. The initial electron state is chosen to scan in the $\varphi = 45^\circ$ plane and a profile of $\Delta(\omega)$ is drawn as a function of θ.

In addition Bennett redrew that $\Delta(\omega)$ profile in the $\varphi = 45^\circ$ plane against θ but with a non-spherical Fermi surface formulated with a four OPW (orthogonal plane wave) approximation [16]. Little difference in $\Delta(\omega)$ was found apart from that in the region around two values of θ where the non-spherical Fermi surface ceases to exist. Bennett concluded that the phonon density of states is the principal source of gap anisotropy.

In 1975 Tomlinson and Carbotte once more evaluated the anisotropy of the superconducting energy gap in lead [19]. They followed the steps of Bennett almost exactly, including the use of Eq. (1) and a non-spherical Fermi surface formulated with the four OPW approximation. Their phonons are from direct evaluation of the Born-von Kármán theory. On the other hand they probably had introduced an approximation in [20] that the end electron state is boldly allowed to run over the interior of a huge phonon sphere that conceptually envelops the entire Fermi surface. They did not evaluate lead gap anisotropy with a spherical Fermi surface for comparison.

In 1971 and 1972 Leavens and Carbotte evaluated gap anisotropy in aluminium, also via Eq. (1) and a non-spherical Fermi surface formulated with one OPW, but did not study the spherical Fermi surface for comparison [21, 22].

In general all the evidence available to us in the literature supports the Bennett conclusion. To our knowledge there is no indication of important contributions to gap anisotropy in metallic superconductors that can be attributed to Fermi surface geometry.

IV. THE EXPERIMENTAL SITUATION

With respect to superconductor anisotropy study the experimental side has been plagued with numerous problems. At one stage the relatively sparse experimental evidence for gap anisotropy was principally from electromagnetic absorption and acoustic attenuation investigations. It appeared in the early 1960's that the newly developed method of electron tunnelling offered the most direct method of energy gap measurement [23]. However interpretation of the tunnelling data needs careful attention, with some issues persisting to this day.

The tunnel structures usually involve the fabrication of thin film sandwiches. There are two regimes. Sufficiently thin films of thickness, d, less than the superconducting coherence length, ξ_0, are polycrystalline with severe boundary scattering and correspondingly short electron mean free paths, a regime classified by Anderson as dirty, and they were expected to show isotropic gaps [15]. Films of greater thickness ($d > \xi_0$) had longer electron mean free paths, were expected to behave as clean systems and should show anisotropy. Townsend and Sutton, in 1962, found evidence in support of Anderson in the case of lead, the element that has been most extensively investigated. They studied two types of tunnel sandwiches: Ta-I-Pb (tantalum-insulator-lead) with a bulk tantalum electrode and entirely thin film Al-I-Pb structures [24].

Later, in 1966-67, in a series of experiments using films of different thicknesses, Campbell and Walmsley further exploited the technique [25]. Thin (dirty, $d < \xi_0$) films were found consistently to show unique gaps while thick ($d > \xi_0$) films showed multiple gaps. In the interpretation the multiple gaps were associated with distinct grains (of dimension $d > \xi_0$) having different preferred orientations in the films and reflecting an anisotropic gap; the idea that multiple gaps could be associated with a single crystallographic direction was recognised but not explored. The anisotropy effects were seen in aluminium, lead, indium and tin. In a separate study by Campbell, Dynes and Walmsley, alloying of lead with bismuth was used to control mean free paths in films of arbitrary thickness and reduction of anisotropy was again established for short mean free path systems [26]. In a contemporaneous study of lead films Rochlin found closely similar results [27].

A little later still, in 1969, Blackford and March overcame previous technical obstacles and investigated tunnelling from epitaxially grown lead single crystals [28]. Using a 1500Å thick lead film as top electrode they reported the energy gap on the faces of lead single crystals in various crystallographic directions. In each direction the gap had a double value which was attributed to two or more groups of electrons coming from different parts

of the Fermi surface of the lead crystal.

By contrast, in 1970 Wells et al examined aluminium crystals by tunnelling from 5000Å-thick aluminium and indium films and reported finding some anisotropy (6%) but no evidence of multiple gaps [29]. In 1971 Lykken et al, building on the work of Wells et al investigated lead single crystal films [30]. Their results did show double gaps in good agreement with Blackford and March. Although they measured top electrode film thicknesses the values are not recorded in detail with the published gap results; they appear typically to have been of the order of 5000Å. Much later, in 2000, Short and Wolfe found evidence in a phonon imaging experiment for what they described qualitatively as large anisotropy in superconducting lead [31].

So, in summary, the experimental electron tunnelling evidence generally has been interpreted as supporting directional anisotropy but is conflicted on whether there are multiple gaps in a single crystallographic direction of a crystal. The latter view is supported by Blackford et al [28] and Lykken et al [30] in lead, by Blackford in aluminium [32] but not by Wells [29] in aluminium. We note in passing that the data in favour all involve thick lead counter-electrodes.

V. BCS DIFFICULTY

We now outline briefly the history that leads to the need for a new pairing scheme in BCS theory. First we observe that it is natural to expect identical phonons in the normal and superconducting states, on account of the BCS premise that the very same electron-phonon interaction is responsible for both electrical resistivity and superconductivity. So, we should not attach particular significance to the black polygons in FIG. 1. Unfortunately each and every attempt along this line of thinking has consistently failed, leaving us with a long trail of evidence in the literature of an unresolved difficulty.

In 1976 Tomlinson and Carbotte [19] evaluated the spectral function $\alpha^2F(\nu)$ for lead with the pseudopotential of Appapillai and Williams which is a specification of the Heine-Abarenkov potential. Ostensible agreement with tunnelling measurement was said to be "very good", although the numerical peak of $\alpha^2F(\nu)$ at 9 meV is more than 2 times as strong as the tunnelling peak. In 1977 Tomlinson and Carbotte [33] in pioneering studies evaluated the normal state resistivity $\rho(T)$ for lead with the same potential. Between $T = 4$ and 295 K their $\rho(T)$ is only about 75% of the observed values, as can be seen clearly from the graphical redrawing of the result in 1981 by Eiling and Schilling [34]. A similar discrepancy occurred when aluminium was investigated using the Heine-Abarenkov potential tabulated by Harrison (where the discrepancy in ρ was somewhat obscured by a logarithmic presentation) [21, 35, 36].

In 1977 Peter, Ashkenazi and Dacorogna determined the effects of anisotropy on the T_c of niobium [37]. They found that the electron-phonon coupling constants determined are probably too large and have to be multiplied by a factor of 0.7 (which, perhaps significantly in the light of later developments, means a factor of 0.49 in the electron-phonon-electron interaction) in order to obtain the observed T_c.

In 1979 Glötzel, Rainer and Schober [38] evaluated $\alpha^2F(\nu)$ for vanadium, niobium, tantalum, molybdenum, tungsten, palladium, platinum and lead. They carefully avoided any uncontrolled approximations. To find phonon dispersion they used published Born-von Kármán fits to the force constants. To estimate the strength of the electron-phonon interaction they used muffin-tin potentials developed for band structure calculation. The superconducting transition temperature they found, T_c, turned out to be 2 to 3 times too high. They showed the value of μ^* has a significant effect on T_c but stuck to a reasonable choice $\mu^* = 0.13$. They concluded that their careful approach was incapable of reproducing the observed values of T_c.

In 1987 Al-Lehaibi, Swihart, Butler and Pinski [39] evaluated both $\rho(T)$ and $\alpha^2F(\nu)$ for tantalum also with a muffin-tin potential from band calculation. While $\rho(T)$ was found to be slightly lower than experimentally observed, $\alpha^2F(\nu)$ exceeded the tunnelling values significantly, giving $T_c = 7.01$ K (4.5 K experimentally) which was regarded as a puzzle [39]. A similar puzzle occurred when niobium was investigated [40–42].

In 1990 Carbotte [43] reviewed the calculations of $\alpha^2F(\nu)$ but surprisingly made no reference to the earlier careful practice of verifying consistency between resistor and superconductor theories via calculations of normal state resistivity $\rho(T)$. The agreement between the numerical and measured tunnelling spectral function $\alpha^2F(\nu)$ for niobium by Butler et al [40] was said to be "not good" (against good numerical ρ) in contrast to the "very good" numerical $\alpha^2F(\nu)$ for lead in [19] (against erroneous numerical ρ).

In 1996 Savrasov and Savrasov [44] evaluated $\rho(T)$ and $\alpha^2F(\nu)$ for aluminium, vanadium, tantalum, lead, niobium, molybdenum, palladium and copper. Their $\rho(T)$ is lower than experiment, significantly in the case of lead, in all cases except for niobium at $T > 300$ K and copper. However their spectral function $\alpha^2F(\nu)$ still exceeds experimental values by a factor of 2 or 3 in places. To reproduce the observed T_c they adjusted μ^* freely without justification. In the case of vanadium and niobium (resistivity largely correct) they let $\mu^* = 0.30$ and 0.21, instead of the measured tunnelling values 0.15 and between 0.11 and 0.16 respectively [45].

In brief, in numerous attempts over more than 20 years the calculated value of the superconducting electron-phonon spectral density, $\alpha^2F(\nu)$, is always found to be too high when the normal state resistivity $\rho(T)$ is reasonable (with the potential from band calculation) or conversely but equivalently $\alpha^2F(\nu)$ is found to be reasonable but $\rho(T)$ is too low (with the Appapillai-Williams or Harrison specifications of the Heine-Abarenkov potential).

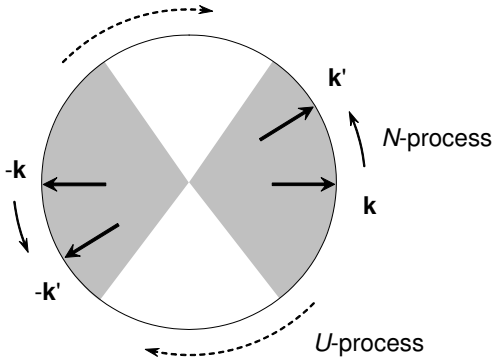

FIG. 2: Schematic of a spherical Fermi surface and a pair of electrons with initial states $\mathbf{k}$ and $-\mathbf{k}$. The end states, $\mathbf{k}'$ and $-\mathbf{k}'$, can be accessed via both normal (N) and umklapp (U) scattering, with different pair occupation probabilities, causing a dilemma.

Since we have little reason to question the theory of normal state electrical resistivity this leaves us no choice but somehow to curtail the strength of the electron-phonon interaction in the superconducting state in order to reproduce experimental tunnelling conductance.

VI. NEW PAIRING SCHEME

How does the BCS difficulty arise? In short: normal and umklapp scattering may compete for the same destination pair states. In normal electron-phonon scattering the end states from $\mathbf{k}$ are restricted to the grey wedge on the right (angle = 78.1°, 60.0°, 51.8°, ... when valency = 1, 2, 3, ...) in FIG. 2 [11]. They can never reach the wedge on the left. End states of umklapp scattering from the same initial state, in contrast, do cover the left wedge [20] and this causes problems.

Specifically in normal scattering an electron in a Cooper pair experiences a transition from $\mathbf{k}$ to $\mathbf{k}'$ (the other electron in the pair scatters from $-\mathbf{k}$ to $-\mathbf{k}'$ by symmetry) giving a destination pair occupation probability $h(\mathbf{k}') = h(-\mathbf{k}')$. In umklapp scattering the transition is from $\mathbf{k}$ to $-\mathbf{k}'$ (the other electron scatters from $-\mathbf{k}$ to $\mathbf{k}'$ by symmetry) giving another distinct destination pair occupation probability $u(\mathbf{k}') = u(-\mathbf{k}')$. In general $h(\mathbf{k}') \neq u(\mathbf{k}')$ because of the different phonons (solid and dashed arrows) involved in the N and U-processes. Should we adopt $h(\mathbf{k}')$ or should we adopt $u(\mathbf{k}')$ when the processes co-exist? That is the dilemma underlying the historical BCS difficulty.

In response we introduce an empirical rule which can be presented analytically as the following interaction survival rate:

$$S(\mathbf{q}) = \begin{cases} 0, & \text{if } \mathbf{k}' \pm \mathbf{k} \text{ is in BZ} \\ 1/2, & \text{otherwise} \end{cases} \qquad (4)$$

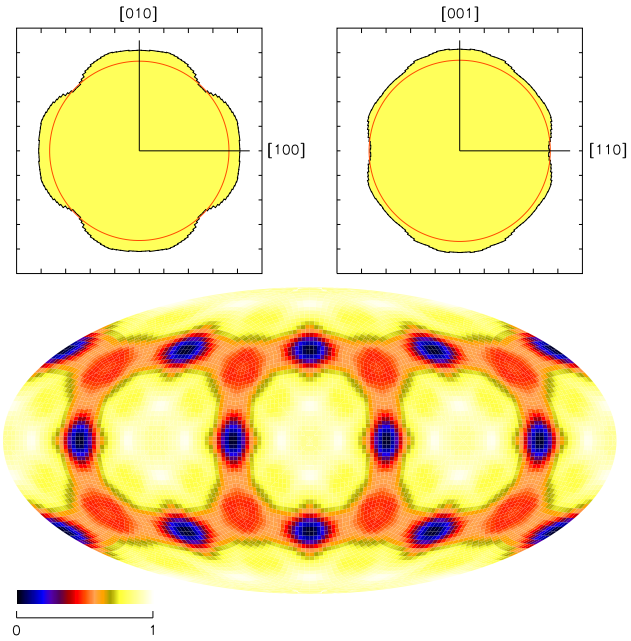

FIG. 3: Gap edge in lead calculated with new pairing scheme. Upper: gap edge profiles in the [001] and [110] planes, circles represent dirty limit. Lower: panoramic map, normalised linear colour scale against minimum gap, standard deviation = 0.15 (in $k_B T_c/2$) or 3.41% of dirty limit, 4.40 (same units) (∼1.365 meV).

where $\mathbf{q} = \mathbf{k}' - \mathbf{k}$ and BZ stands for the first phonon Brillouin zone shown in FIG. 1 as the black areas; $S(\mathbf{q}) \equiv 1$ for the BCS scheme. The rule weights the strength of the electron-phonon interaction and hence curtails the contribution to $\alpha^2F(\nu)$ of that interaction. Clearly Eq. (4) helps to circumvent the BCS conceptual difficulty; see [9, 10] for detailed microscopic justifications. In a series of publications we established the worth of Eq. (4) in that it allows the same pseudopotential to be used to evaluate the electron-phonon interaction for both normal state resistivity and superconductivity with high accuracy [9, 10, 12, 13]. Indeed it becomes clear that the new pairing potential is much better in that it is close to the resistivity-derived potential and contrasts with the BCS potential.

VII. LEAD: TWO PAIRING SCHEMES

We describe briefly the numerical procedure for solving Eq. (1). Interested readers may consult [46] for further details. We start by determining the lead phonon dispersion curves. For lead this used to be seen as a difficult task and led Chen and Overhauser to suspect involvement of spin-density waves in 1988 [47] but a test experiment by Overhauser and Giebultowicz gave a null result in 1993 [48]. We solved the problem within the

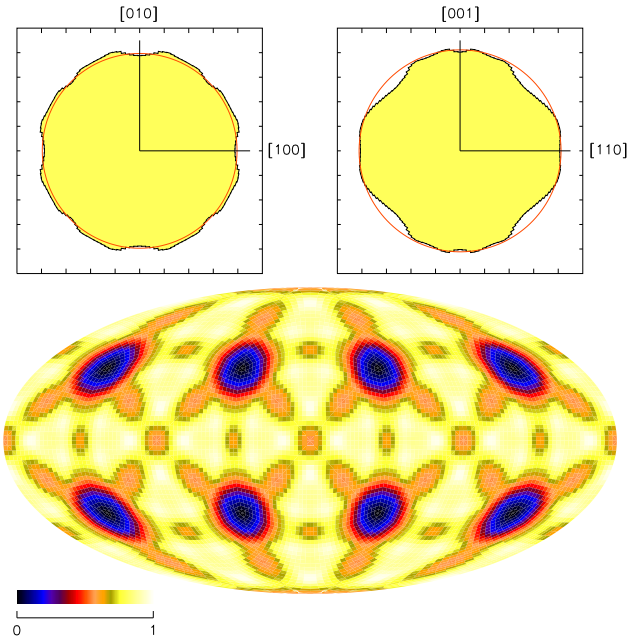

FIG. 4: Gap edge in lead calculated with BCS pairing scheme. Upper: gap edge profiles in the [001] and [110] planes, circles represent dirty limit. Lower: panoramic map, normalised linear colour scale against minimum gap, standard deviation = 0.16 (in $k_B T_c/2$) or 3.64% of dirty limit, 4.40 (in same units) ($\sim$1.365 meV).

TABLE I: SUMMARY OF PSEUDOPOTENTIAL PARAMETERS

Element	potential	theory	r_1/a	$\delta V/\epsilon_F$	error[a]
		resist	0.834	-3.408	0.12%
Pb	muffin-tin	new	0.790	-3.773	
		BCS	0.369	-1.651	
		resist	0.413	-2.669	0.69%
Al	Gaussian	new	0.389	-2.721	
		BCS	0.333	-1.066	
		resist	0.999	-4.087	0.38%
Nb	muffin-tin	new	1.110	-3.773	
		BCS	0.419	-1.781	
		resist	1.004	-4.556	0.55%
Ta	muffin-tin	new	1.084	-4.297	
		BCS	0.448	-1.833	

[a] against ρ at 295K

framework of the Born-von Kármán theory with a force model having central symmetry across 20 neighbouring atomic shells. In this model, at each atomic shell, the force constant matrix arises from a pair of parameters: we have a total of 40 parameters to determine.

We follow the numerical procedure of direct search due to Hooke and Jeeves [49] to determine the 40 or so parameters of the central force model. There is no strict linkage between the number of atomic shells and the size of the experimental dataset. In the pattern search phase of the procedure the 40 parameters of the force model are perturbed in turn. A perturbation is registered as positive if it improves fitting between theory and experiment, otherwise it is registered as negative. In the pattern move phase all the positive perturbations are performed simultaneously, negative perturbations are performed simultaneously in opposite directions, to the extent needed for best fitting. This procedure is repeated until the fit no longer improves [46].

TABLE II: LEAD ENERGY GAP [a]

	[100]	[110]	[111]	std dev	%[b]
Experimental					
Blackford	4.19	4.23	4.15	0.03	0.78
Lykken	4.14	4.25	4.15	0.05	1.19
Previously calculated					
Bennett	4.69	4.04	4.44	0.27	6.10
Tomlinson[c]	4.21	5.01	4.23	0.37	8.31
Currently calculated					
New pairing scheme	4.94	4.36	4.66	0.24	5.09
BCS scheme	4.31	4.35	3.93	0.19	4.51

[a] in $k_B T_c/2$ with $T_c = 7.193K$
[b] against average gap in the row
[c] approximate directions

In the normal state we use Eq. (3) to evaluate $\alpha^2_{\rm tr}F(\nu)$, that in turn is used to evaluate the extended version of the Mott-Jones equation for electrical resistivity, assumed to be isotropic, and umklapp scattering is included. Calculated values of resistivity are compared with the experimental data and the parameters r_1 and δV in Eq. (3) are adjusted via the Hooke-Jeeves procedure for a best fit, see [50] for further details. We could refine the shape of the muffin-tin potential in Eq. (3) for better fitting, but chose not to do so due to the sheer amount of calculations involved. The calculation is sufficiently accurate with $r_1 = 0.834a$ and $\delta V = -3.408\epsilon_F$, a being the crystal constant and ϵ_F Fermi energy. On average the calculated resistivity differs from measurement by just 0.12% of the lead resistivity at 295 K. For convenience of reference we present these and other pseudopotential parameters determined in the course of the present work in Table I.

In the superconducting state Eq. (3) is used to evaluate $\alpha^2F(\nu)$ which in turn is used to evaluate Eq. (1). We apply the new pairing scheme, in which the electron-phonon interaction contributes to superconductivity only when the end states of the scattered electron fall beyond the black regions in FIG. 1. The strength of the surviving interaction is, as in all our previous related publications, also halved. We first find the dirty limit, $\overline{\Delta}(\omega)$, via the Hooke-Jeeves procedure for best fitting. En route we determine μ^* in Eq. (2), see [12] for details.

Equipped with $\alpha^2F(\nu)$, the dirty limit of the gap and

μ^* for lead, it is straightforward to find the anisotropic gap from Eqs. (1) and (2). We see from TABLE II that in the outcome for lead we have the maximum value of the gap edge in the [100] direction, a lower value along [110] and an intermediate value along [111]. These are shown in the upper part of FIG. 3. In the lower part of FIG. 3 we map values of the gap edge globally over the Fermi surface with 20160 pixels.

Next, out of interest and for comparison we switch to the usual BCS pairing scheme by allowing both normal and umklapp scattering to contribute to superconductivity, regardless of whether the end states in FIG. 1 fall within or beyond the black regions. Calculated tunnelling conductance fits experimental data reasonably well, though not as well as found with the new pairing scheme. The atomic potential weakens significantly, with $r_1 = 0.369a$ and $\delta V = -1.651\epsilon_F$, in order to accommodate additional contributions by normal electron-phonon scattering in the original BCS scheme.

Anisotropy of the energy gap also changes pattern significantly under the BCS scheme. In TABLE II the maximum value of the gap edge is now in the [110], direction, with a lower value in the [100] direction and a lower still value along [111]. This appears to suggest a rotation of 45° from the 4 lobes of the gap profile in the [001] plane for the calculation with the new pairing scheme in the upper part of FIG. 3. We see from the upper part of FIG. 4 that in the [001] plane the gap profile calculated with the BCS pairing scheme has 8 lobes with reduced amplitudes. The global map in the lower part of FIG. 4 also changes significantly in comparison with the map in FIG. 3. In general the magnitude of the anisotropy is broadly comparable in both calculations. The difference between the two pairing schemes lies most obviously in the pattern of the gap edge in the [001] plane.

VIII. LEAD: REVIEW OF PREVIOUS RESULTS

Experimentally the energy gap in lead single crystals was reported to have two (sometimes three) values, reflecting fine structure in the tunnelling current. It was said to be due to two (or more) groups of tunnelling electrons coming from different parts of the Fermi surface of the crystal [28, 30]. (Such structure was not found in aluminium single crystals by Wells [29]).

Before accepting this view at face value it is worth looking again at the experimental evidence and its interpretation. The tunnel sandwiches consisted of an epitaxially grown single crystal as one electrode and an evaporated film as the other. In their case, Blackford and March report that the top film is 1500Å thick [28]. In lead the coherence length is $\xi_0 = 830$Å so these films fall into the thick category. They are expected to have grains with dimensions of the same order as the film thickness and should show multiple gaps according to earlier studies [26, 27]. Inspection of the data suggests that the double gaps observed can be attributed to the top film electrode with a cluster of values at 2.45 meV and another at 2.77 meV. If we attribute the multiple gaps to the top film exclusively then the mean value in each case corresponds to the gap of the single crystal. It varies from 2.60 meV by at most 0.03 meV or 1% from one direction to another. This implies only weak anisotropy in the single crystal. Later, Lykken et al used lead films of thickness approaching 5000Å and again multiple gaps should arise therefrom. These were indeed observed and the results were interpreted in the Blackford fashion. However, with the alternative attribution of the multiple gaps and anisotropy to the top film the crystal gap again is unique in each crystallographic direction and varies in different directions from 2.60 meV by only 0.03 meV. The film gaps cluster around 2.40meV and 2.75 meV. By contrast, in the case of aluminium studied by Wells et al the counter-electrode used was 5000Å thick, much less than the coherence length in aluminium ($\xi_0 = 16,000$Å) and therefore multiple gaps were not expected here in the top film nor were they observed in the experiment [29].

With this revised interpretation the experimental evidence points to modest anisotropy in lead single crystals, perhaps 1%. There is good consistency between the measurements reported by the two research groups for the [111] and [110] directions as summarised in TABLE II though slightly less so for the [100] direction [28, 30]. On the other hand, theory suggests, as seen in TABLE II, anisotropy magnitudes of 5 to 8% [16, 51]. The discrepancy is dramatic.

Tomlinson and Carbotte [51] highlighted some consistency between their calculations and the earlier interpretation of the experiment of Blackford [28] because in both cases the gap peaks about two values. However, the current discussion questions that interpretation of the experimental data. The difference between FIG. 3 here and the result of Tomlinson and Carbotte in [51] will in part reflect the details of the pairing scheme. They will have adopted the original BCS pairing scheme, together with their procedure of including umklapp scattering to calculate phonons in an enlarged sphere that conceptually envelopes the entire Fermi sea [20]. Indeed we see from TABLE II and FIG. 4 that choice of pairing does make a significant difference in gap anisotropy variation and the trends seen by Tomlinson and Carbotte are reflected there: maximum gap along [110], minimum along [100] and intermediate along [111]. The relative impact of electron band structure which they also included is hard to quantify.

From TABLE II the theory of Bennett [16] appears, rather unexpectedly, to show the same general trend as the results of our calculations based on the new pairing scheme in FIG. 3 though there are numerical discrepancies: the maximum gap is in the [100] direction, a lesser gap is found in [110] and an intermediate gap along [111]. Indeed in FIG. 8 in [16] the gap profile in the [110] plane resembles closely the corresponding profile in the upper part of FIG. 3 here. We refrain from reading too much into this, because Bennett applied rather bold approxi-

TABLE III: ALUMINIUM ENERGY GAP[a]

	[100]	[110]	[111]	std dev	%[b]
Experimental					
Biondi	3.44	3.37	3.50	0.05	1.55
Kogure	3.56	3.46	3.14	0.18	5.29
Blackford	3.38		2.69	0.35	11.4
Wells	3.64		3.41	0.12	3.26
Previously calculated					
Dynes	3.78	3.68	3.39	0.17	4.57
Leavens	3.64	3.51	2.93	0.31	9.19
Leung	3.32	3.27	3.11	0.09	2.77
Currently calculated					
New pairing scheme	3.93	3.24	3.17	0.34	10.0
BCS scheme	3.54	3.57	3.08	0.22	6.60

[a] in $k_BT_c/2$ with $T_c = 1.25K$
[b] against average gap in the row

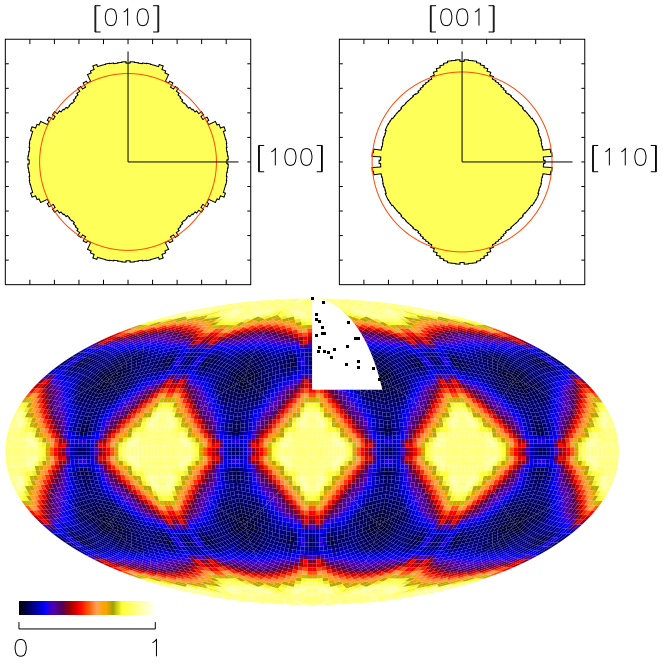

FIG. 5: Gap edge in aluminium, new pairing scheme. Upper: gap edge profiles in the [001] and [110] planes, circles represent dirty limit. Lower: panoramic map, normalised linear colour scale against minimum gap, standard deviation = 0.29 (in $k_BT_c/2$) or 8.24% of dirty limit, 3.52 (same units) ($\sim$ 0.1895 meV). Blackford sample points shown in the clear sector.

mations in his calculation. For example in [16] the form of $\alpha^2F(\nu)$ is assumed to be a Lorentzian, with parameters adjusted to fit an experiment in the normal state.

The overall tentative conclusion for lead is that theory and experiment are in serious disagreement. The experimental anisotropy data from tunnelling into single crystals is in magnitude (1%) well short of theoretical prediction (5-8%).

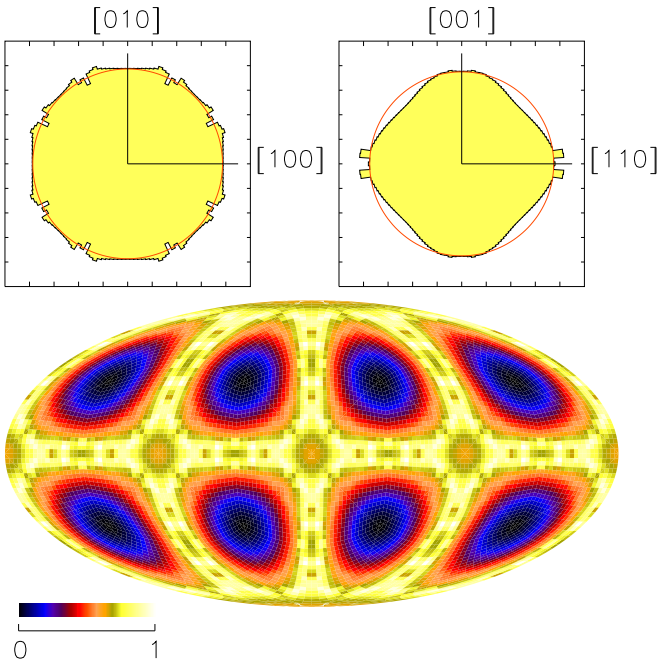

FIG. 6: Gap edge in aluminium, BCS pairing scheme, Upper: gap edge profiles in the [001] and [110] planes, circles represent dirty limit. Lower: panoramic map, normalised linear colour scale against minimum gap, standard deviation = 0.20 (in $k_BT_c/2$) or 5.67%, of dirty limit, 3.52 (same units) ($\sim$ 0.1895 meV).

IX. ALUMINIUM

Study of the superconducting energy gap in aluminium has been a central focus of the electron tunnelling technique since the beginning but the low transition temperature, 1.196 K reported by Wells et al [29] and 1.180 K by Blackford [32], made reliable superconductivity measurement challenging. Experimentally the gap edge was found to be 2.3 ± 0.3 (in $k_BT_c/2$) at 0.8 K by Nicol, Shapiro and Smith in 1960 [52], 3.20 ± 0.30 at 1 K by Giaever and Megerle in 1961 [23] and finally an asymptotic value of 3.53 ± 0.02 at absolute zero, transition temperature = 1.250 K, by Blackford and March in 1968 [53]. Beware that for some reason it is still often listed as 3.3 in popular textbooks [54].

Study of anisotropy of the gap in aluminium also started early. Experimentally, Biondi et al in 1964 had found anisotropy via millimeter-microwave studies and Claiborne and Morse detected considerable difference in attenuation of ultrasonic shear waves in a superconducting aluminium single crystal in the [100], [110] and [111] directions [55, 56]. With the latter technique Kogure et al found the maximum gap in [100], a lower value in [110] and least in [111] [57]. Blackford and Wells et al carried out tunnelling measurements and found results consistent with these relative values, see TABLES II and III [29, 32]. Early theoretical contributions were made by

TABLE IV: ALUMINIUM ENERGY GAP[a]

θ	φ	Blackford[b]	new[c]	BCS[d]
0.0	0.0	3.38	3.97 (0.59)	3.54 (0.16)
5.6	30.9	3.25	3.96 (0.71)	3.55 (0.30)
16.4	5.7	3.53	3.97 (0.44)	3.65 (0.12)
19.8	5.6	3.53	3.91 (0.38)	3.65 (0.12)
21.6	8.6	3.34	4.01 (0.67)	4.86 (1.52)
22.4	39.0	3.18	3.70 (0.52)	3.50 (0.32)
25.6	10.2	3.43	3.77 (0.34)	3.67 (0.24)
29.3	11.7	3.57	3.61 (0.04)	3.65 (0.08)
29.4	9.2	3.58	3.68 (0.10)	3.73 (0.15)
30.6	4.1	3.53	3.69 (0.16)	3.79 (0.26)
32.1	40.8	3.12	3.40 (0.28)	3.37 (0.25)
32.5	37.5	3.53	3.39 (0.14)	3.37 (0.16)
37.1	28.6	3.58	3.34 (0.24)	3.35 (0.32)
37.3	5.7	3.06	3.66 (0.60)	4.02 (0.96)
38.5	18.1	3.05	3.30 (0.25)	3.46 (0.41)
39.8	5.2	3.68	3.24 (0.44)	3.54 (0.14)
39.9	9.4	2.91	3.29 (0.38)	3.58 (0.67)
40.6	12.4	2.66	3.27 (0.61)	3.53 (0.87)
43.3	14.7	3.23	3.18 (0.05)	3.47 (0.24)
45.4	33.9	3.25	3.25 (0.00)	3.20 (0.05)
46.9	24.8	3.40	3.24 (0.16)	3.29 (0.11)
48.3	32.5	2.79	3.24 (0.45)	3.19 (0.40)
48.9	43.1	3.71	3.20 (0.51)	3.11 (0.60)
54.7	45.0	2.69	3.19 (0.50)	3.08 (0.39)

[a] angle in degrees, gap in $k_BT_c/2$, deviation bracketed
[b] experimental, average gap = 3.29
[c] new scheme, average gap (deviation) = 3.52 (0.36)
[d] BCS scheme, average gap (deviation) = 3.55 (0.37)

Carbotte and collaborators [21, 36, 58].

In order to calculate the anisotropy in aluminium within our model we proceed much as before. Specifically we evaluate Eq. (1) for aluminium as we did the equation for lead in Section VII, apart from the fact that we find we now have to replace the muffin-tin potential in Eq. (3) with the following Gaussian potential:

$$V(r) = \delta V \exp\left[-\left(\frac{r}{r_1}\right)^2\right] \tag{5}$$

which we apply to calculate $\alpha^2F(\nu)$ in Eq. (2) [46]. We find $r_1 = 0.389a$ and $\delta V = -2.721\epsilon_F$ in the superconducting state with the new pairing scheme, compared with $r_1 = 0.333a$ and $\delta V = -1.066\epsilon_F$ with the BCS formulation. We also find $r_1 = 0.413a$ and $\delta V = -2.669\epsilon_F$ for the normal state with average error = 0.69% in normal state electrical resistivity between 0 and 295 K compared with the value of resistivity at 295 K.

With the new pairing scheme, the outcomes of our calculation demonstrate a clear pattern of gap anisotropy: a maximum in the [100] direction, a lower value along [110] and a lower still value along [111], as is shown clearly in TABLE III and FIG. 5. The tunnelling data from several experimental groups [29, 32, 57], also shown in TABLE III, demonstrate a consistent dominant pattern, despite significant differences in absolute values of the data. The Biondi microwave data are the least compatible [56]. Overall we are encouraged by the comparison between experiment and theory.

On the other hand, with the usual BCS pairing scheme, it is clear from TABLE III that the maximum value of the aluminium gap edge is in the [110] direction, with a slightly lower value along [100] and a lower still value along [111], which is closely similar to the pattern of lead anisotropy in TABLE II calculated with the BCS pairing scheme. We see from the upper part of FIG. 6 that, now, the aluminium gap profile in the [001] plane has 8 lobes with reduced amplitudes, similar to the lead gap profile in the [001] plane in the upper part of FIG. 4.

Blackford measured the values of the aluminium gap edge in numerous other directions [32], as illustrated in the clear sector in the lower part of FIG. 5, data listed in TABLE IV. We show calculated aluminium gap edge values in each direction, with both the new and usual BCS pairing schemes, also in TABLE IV. On average the Blackford data yield a gap edge 3.29 (in $k_BT_c/2$), compared with 3.52 (0.36 average deviation) from the new pairing scheme and 3.55 (0.37 average deviation) from the BCS scheme. The experimental gap appears to be too low (should be ∼3.53) [53] possibly due to measurement difficulty rather than sample selection, considering the fairly random distribution of the sample points in the clear sector in the lower part of FIG. 5.

TABLE V: NIOBIUM ENERGY GAP[a]

	[100]	[110]	[111]	std dev	%[b]
Experimental					
Dobbs	3.77	3.68	3.74	0.04	1.00
MacVicar	3.59	3.91	4.02	0.18	4.75
Bostock	3.93	3.93	3.93	0.00	0.00
Hahn	2.91	4.01	4.37	0.62	16.5
Currently Calculated					
New pairing scheme	4.10	3.34	3.86	0.32	8.42
BCS scheme	4.37	2.92	4.24	0.65	17.0

[a] in $k_BT_c/2$ with $T_c = 9.50K$
[b] against average gap in the row

X. NIOBIUM

Electron tunnelling measurement of gap anisotropy in niobium has a long and unsettled history. In a careful study in 1973 Bostock et al [59] conducted tunnelling experiments on niobium single crystals in 26 directions, with carefully prepared indium and lead-bismuth counter-electrodes, only to detect no anisotropy, see TABLE V. This conclusion overrode earlier outcomes such as the 1967 MacVicar and Rose study [60] which conducted superconducting tunnelling experiments on niobium single crystals in 6 directions and found a minimum gap in the [100] direction, an intermediate value in [110] and large values in [111] and [311], see TABLE V. Later, in 1969 MacVicar [61] conducted similar experiments in

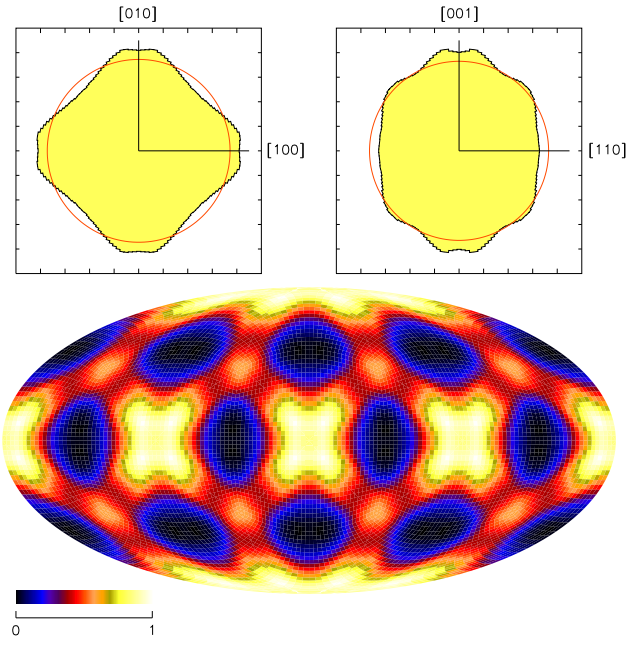

FIG. 7: Gap edge in niobium, new pairing scheme, Upper: gap edge profiles in the [001] and [110] planes, circles represent dirty limit. Lower: panoramic map, normalised linear colour scale against minimum gap, standard deviation = 0.25 (in $k_BT_c/2$) or 6.70% of dirty limit, 3.73 (same units) ($\sim$ 0.1525 meV).

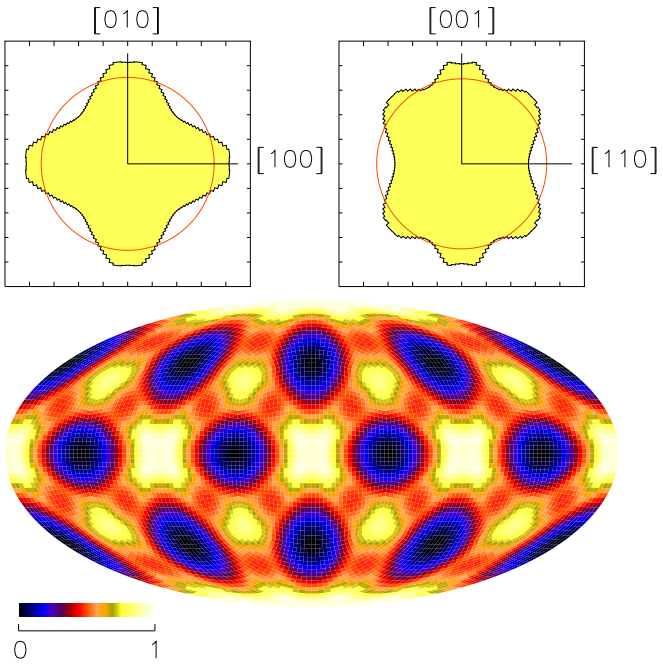

FIG. 8: Gap edge in niobium, BCS pairing scheme,Upper: gap edge profiles in the [001] and [110] planes, circles represent dirty limit. Lower: panoramic map, normalised linear colour scale against minimum gap, standard deviation = 0.40 (in $k_BT_c/2$), or 10.7% of dirty limit, 3.73 (same units) ($\sim$0.1525 meV).

numerous directions and found gap values grouped non-randomly in **k**-space. The final view was that there is no observed anisotropy.

In 1962 in mild support of this conclusion Townsend and Sutton found no clear evidence of anisotropy or multiple gaps in a tunnelling study of zone-refined ingots of niobium [24]. The coherence length, ξ_0, in niobium is 380Å and the grain size in zone-refined ingots might be expected to exceed this value, in which situation anisotropy should be observable. In 1980 Wolf and co-workers, too, reported isotropic measurements from thin niobium films [62].

But other authors do report anisotropy in superconducting niobium. In 1964 Dobbs and Perz [63] found niobium gap anisotropy from ultrasonic measurements, with a maximum in the [100] direction, minimum along [110] and an intermediate value along [111], see TABLE V, that is characteristically different from the result of Hahn et al [64] because now the gap edge in the [100] direction is no longer a minimum, indicative of a 45° rotation of the gap profile in the [001] plane. Theoretical calculations by Daams and Carbotte also demonstrate anisotropic gaps in niobium [65] but with scarcely further details.

In 1983 Durbin et al [66] measured tunnelling current in niobium single crystals in the [100] and [111] directions over an extensive range of applied voltages, in order to recover $\alpha^2F(\nu)$ via McMillan inversion. In principle this would have allowed them to find the gap edges numerically but the inversion program failed to converge for the [111] data. Unfortunately they did not report a directly measured gap from conductance characteristics. In 1998 Hahn et al [64] adopted a similar approach, involving the Andreev approximation and Bogoliubov-De Gennes equation, and found gap edges in [001], [110] and [111] with large anisotropy, see TABLE V.

For niobium our evaluation of Eq. (1) is similar to that for lead in Section VI. We find $r_1 = 0.999a$ and $\delta V = -4.087\epsilon_F$ in the normal state, average error = 0.38% for electrical resistivity between 0 and 295 K, compared with the value of resistivity at 295 K. For the new pairing scheme we find $r_1 = 1.110a$ and $\delta V = -3.773\epsilon_F$. We find a pattern of anisotropic gap edge in niobium with a maximum in the [100] direction, lower value along [111] and least along [110], see TABLE V and FIG. 7. This pattern is similar to that found experimentally by Dobbs and Perz [63] but the magnitude calculated is much greater than that measured.

For the usual BCS pairing scheme there is little change in superconducting niobium gap anisotropy: we still have the maximum gap edge in the [100] direction, lower value along [111] and least along [110], but gap amplitude varies more significantly, see TABLE V and FIG. 8.

Hahn et al argued in an overview, see [64] and the references therein, that successful anisotropy measurement

TABLE VI: TANTALUM ENERGY GAP[a]

	[100]	[110]	[111]	std dev	%[b]
Experimental					
Sarafi	3.32	3.34		0.01	0.30
Currently Calculated					
New pairing scheme	4.12	3.39	3.61	0.31	8.25
BCS scheme	4.33	3.02	4.17	0.58	15.2

[a] in $k_B T_c/2$ with $T_c = 4.483K$
[b] against average gap in the row

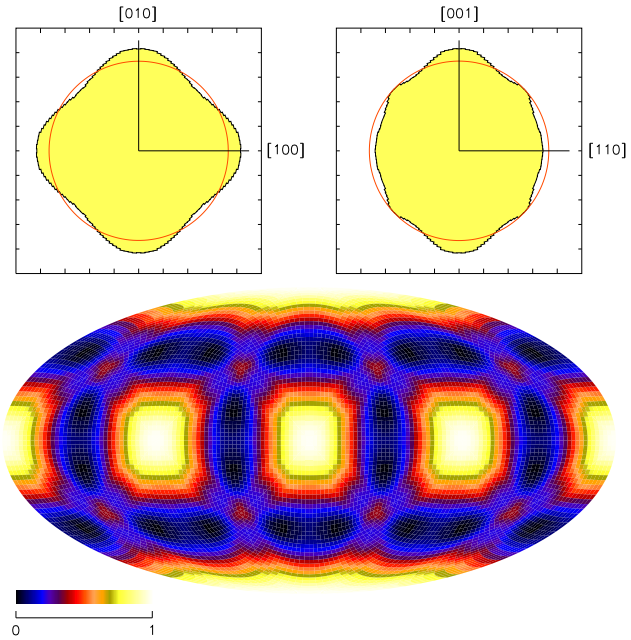

FIG. 9: Gap edge in tantalum, new pairing scheme. Upper: gap edge profiles in the [001] and [110] planes, circles represent dirty limit. Lower: panoramic map, normalised linear colour scale against minimum gap, standard deviation = 0.22 (in $k_B T_c/2$), or 6.08% of dirty limit, 3.62 (same units) ($\sim$ 0.7 meV).

can be expected only with strong forward focusing tunnel injection through a barrier, characterised by a low magnitude of transmission probability, $D \sim 10^{-8}$. In reality D can be much greater and for aluminium-oxide barriers used on niobium for proximity electron tunnelling, D is between 0.01 and 0.1 or even close to unity, 6 to 8 orders above the maximum D for gap anisotropy detection.

XI. TANTALUM

In 1962 Townsend and Sutton found no anisotropy from tunnelling in zone-refined tantalum ingots [24]. In 1968 Sarafi [67] measured gap anisotropy in tantalum single crystals by means of ultrasonic attenuation. Only two directions in the [001] plane were measured and the

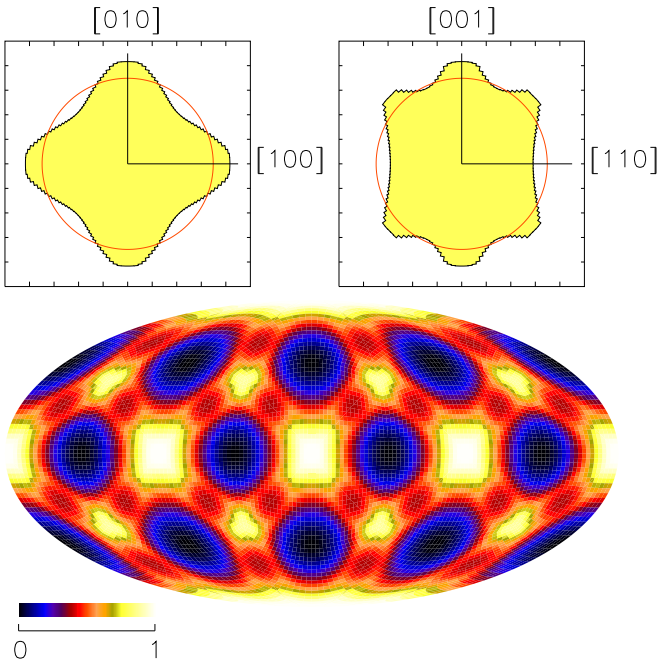

FIG. 10: Gap edge in tantalum, BCS pairing scheme. Upper: gap edge profiles in the [001] and [110] planes, circles represent dirty limit. Lower: panoramic map, normalised linear colour scale against minimum gap, standard deviation = 0.34 (in $k_B T_c/2$), or 9.39% of dirty limit, 3.62 (same units) ($\sim$ 0.7 meV).

result appears to indicate scarcely any anisotropy, see TABLE VI.

Our evaluation of Eq. (1) for tantalum is similar to that for lead in Section VI, with $r_1 = 1.084a$ and $\delta V = -4.297\epsilon_F$ for the new pairing scheme, compared with $r_1 = 0.448a$ and $\delta V = -1.833\epsilon_F$ for the BCS scheme. We also find $r_1 = 1.004a$ and $\delta V = -4.556\epsilon_F$ in the normal state, average error = 0.55% for electrical resistivity between 0 and 295 K, compared with the value of resistivity at 295 K.

Under the new pairing scheme we found a maximum gap in the [100] direction, a substantially lower value along [110] and an intermediate value along [111], see TABLE VI and FIG. 9. Once more phonon-induced anisotropy (8%) from calculation turns out to be much greater than reported in the sparse experimental data in the open literature.

For the usual BCS pairing scheme there is little change in superconducting tantalum gap anisotropy: we still have the maximum gap edge in the [100] direction, lower value along [111] and least along [110], but gap amplitude varies more significantly, see TABLE VI and FIG. 10.

XII. CONCLUSIONS

Previous anisotropy studies of conventional superconductors have been far from satisfying or conclusive. The underpinning Bennett theory has not been adequately evaluated. Furthermore, the experimental measurements on single crystals have offered sparse and sometimes confusingly conflicting data which are inadequate to discriminate between theories. Indeed the question arises as to whether or not electron tunnelling spectroscopy can reveal single crystal anisotropy. In this article the Bennett theory is numerically evaluated and the gap displayed visually for all directions in **k**-space with high resolution for the fcc metals lead and aluminium and bcc metals niobium and tantalum. Conditions required by the theory are carefully observed. The Bennett conclusion that phonon anisotropy is the principal source of gap anisotropy is adopted and a spherical Fermi surface is assumed. A comparison is made between the predicted gap values in the usual BCS scheme of electron pairing and those of a new scheme that rectifies a fundamental inadequacy in the BCS theory. A generic pattern of anisotropy is found with the new scheme: the maximum gap value lies in the [100], [010] and [001] directions, exceeding the minimum by 5 - 8%. The profile of the gap edge in the [001] plane always has 4 lobes reminiscent of a mixture of s and d-wave patterns. In contrast this profile has 8 lobes with the BCS scheme in the fcc metals. We can hope to see an experimental determination of this pattern in real metals to resolve the question of whether the new pairing scheme is supported. Magnesium diboride, MgB_2, a conventional superconductor with T_c of 39K has previously been analysed numerically by Choi et al [68] with the BCS pairing scheme in terms of its isotropic properties. It will be interesting and challenging to analyse its anisotropic properties with both pairing schemes both numerically and experimentally [69, 70].

[1] A. P. Drozdov, M. I. Eremets, I. A. Troyan, V. Ksenofontov and S. I. Shylin, Conventional superconductivity at 203 Kelvin at high pressures in the sulfur hydride system, Nature **525** (2015) 73.

[2] J. Bardeen, L. N. Cooper and J. R. Schrieffer, Theory of superconductivity, Phys. Rev. **108** (1957) 1175.

[3] G. M. Eliashberg, Interactions between electrons and lattice vibrations in a superconductor, JETP **38** (1960) 966. Trans: Soviet Physics JETP **11** (1960) 689.

[4] A.P. Durajski, R. Szczesniak and L. Pietronero, High-temperature study of superconducting hydogen and deuterium sulfide, Ann. Phys. **528** (2015) 358.

[5] Yinwei Li, J. Hao, H. Liu, Yanling Li and Y Ma, The metallization and superconductivity of dense hydrogen sulfide, J. Chem. Physics **140** (2014) 174712.

[6] J. E. Hirsch, BCS theory of superconductivity: it is time to question its validity, Phys. Scr. **80** (2009) 035702.

[7] A. P. Durajski, R. Szkześniak, Y. Li, Non-BCS thermodynamic properties of H_2S superconductor, Physica C **515** (2015) 1.

[8] A.P. Durajski, Quantitative analysis of nonadiabatic effects in dense H3S and PH3 superconductors, Sci. Rep. **6** (2016) 38570.

[9] X. H. Zheng and D. G. Walmsley, Empirical rule to reconcile BCS theory with electron-phonon interaction in normal state, Phys. Scr. **89** (2014) 095803.

[10] X. H. Zheng and D. G. Walmsley, BCS theory has to be overhauled: reassurance from numerical survival rate, Solid State Comm. **237-238** (2016) 42.

[11] X. H. Zheng and D. G. Walmsley, New pairing scheme to overhaul BCS theory, Solid State Comm. **192** (2014) 56.

[12] X. H. Zheng and D. G. Walmsley, Further test of new pairing scheme used in overhaul of BCS theory, Physica C **506** (2014) 100.

[13] X. H. Zheng and D. G. Walmsley, Discrepancy between theory and measurement of superconducting vanadium, Physica C **515** (2015) 41.

[14] R. Joynt and L. Taillefer, The superconducting phases of UPt_3, Rev. Modern Phys. **74** (2002) 235.

[15] P. W. Anderson, Theory of Dirty Superconductors, J. Phys. Chem. Solids **11** (1959) 26.

[16] A. J. Bennett, Theory of the anisotropic energy gap in superconducting lead, Phys. Rev. **140** (1965) A1902.

[17] J. P. Carbotte and R. C. Dynes, Superconductivity in simple metals, Phys. Rev. **172** (1968) 476.

[18] B. T. Geilikman and V. Z. Kresin, Effect of anisotropy on the properties of superconductors, Soviet Phys. JETP **5** (1964) 2605.

[19] P. G. Tomlinson and J. P. Carbotte, Anisotropic superconducting energy gap in Pb, Phys. Rev. B **13** (1976) 4738.

[20] J. P. Carbotte and R. C. Dynes, Superconductivity in simple metals, Phys. Rev. **172** (1968) 476.

[21] C. R. Leavens and J. P. Carbotte, Anisotropic energy gap in Al, Solid State Commun. **9** (1971) 75.

[22] C. R. Leavens and J. P. Carbotte, Gap anisotropy in a weak coupling superconductor, Ann. Phys. **70** (1972) 338.

[23] I. Giaever and K. Megerle, Study of superconductors by electron tunnelling, Phys. Rev. **122** (1961) 1101.

[24] P. Townsend and J. Sutton, Investigation by electron tunnelling of the superconducting energy gaps in Nb, Ta, Sn and Pb, Phys. Rev. **128** (1962) 591.

[25] C. K. Campbell and D. G. Walmsley, Tunnelling investigation of energy-gap anisotropy in superconductors, Can. J. Phys. **45** (1967) 159.

[26] C. K. Campbell, R. C. Dynes and D. G. Walmsley, Anisotropy of the energy gap in superconducting lead-bismuth alloys, Can. J. Phys. **44** (1966) 2601.

[27] G. I. Rochlin, Determination of the anisotropy of the energy gap in superconducting Pb by superconductive tunnelling, Phys. Rev. **153** (1967) 513.

[28] B. L. Blackford and R. H. March, Tunnelling investigation of energy-gap anisotropy in superconducting bulk Pb, Phys. Rev. **186** (1969) 397.

[29] G. L. Wells, J. E. Jackson and E. N. Mitchell, Superconducting tunnelling in single crystal and polycrystal films of aluminium, Phys. Rev. B **1** (1970) 3636.

[30] G. L. Lykken, A. L. Geiger, K. S. Dy and N. Mitchell, Measurement of the superconducting energy gap and Fermi velocity in single-crystal lead films by electron tunnelling, Phys. Rev. B **4** (1971) 1523.

[31] J. D. Short and J. P. Wolfe, Evidence for large gap anisotropy in superconducting Pb film from phonon imaging, Phys. Rev. Lett. **85** (2000) 5198.

[32] B. L. Blackford, A tunnelling investigation of energy-gap, anisotropy in superconducting bulk aluminium crystals, J. Low Temp. Phys. **23** (1976) 43.

[33] P. G. Tomlinson and J. P. Carbotte, Multiple plane wave calculation of the resistivity of Pb and dilute Pb alloys, Can. J. Phys. **55** (1977) 751.

[34] A. Eiling and J. S. Schilling, Pressure and temperature dependance of electrical resistivity of Pb and Sn from 1-300 K and 0-10 GPa − use as continuous resistive pressure monitor accurate over wide temperature range; superconductivity under pressure in Pb, Sn and In, J. Phys. F: Metal Phys. **11** (1981) 623.

[35] P. T. Truant and J. P. Carbotte Electron-phonon scattering times for aluminium, Can. J. Phys. **52** (1974) 618.

[36] H. K. Leung, J. P. Carbotte and C. R. Leavens, Multiplane-wave theory of gap anisotropy in Al, J. Low Temp. Phys. **24** (1976) 25.

[37] M. Peter, J Ashkenazi and M Dacorogna, Unrestricted solution of the Eliashberg equations for Nb, Helv. Phys. Acta **50** (1977) 267.

[38] D. Glötzel, D. Rainer and H. R. Schober H R, Ab initio calculation of the superconducting transition temperature, Z. Physik **35** (1979) 317.

[39] A. Al-Lehaibi, J. C. Swihart, W. H. Butler and F. J. Pinski, Electron-phonon interaction effects in tantalum, Phys. Rev. B **36** (1987) 4103.

[40] W. H. Butler, H. G. Smith and N. Wakabayashi, Electron-phonon contribution to phonon linewidth in Nb: theory and experiment, Phys. Rev. Lett. **36** (1977) 1004.

[41] W. H. Butler, F. J. Pinski and P. B. Allen, Phonon linewidth and electron-phonon interaction in Nb, Phys. Rev. B **19** (1979) 3708.

[42] F. J. Pinski, P. B. Allen and W. H. Butler, Calculated electrical and thermal resistivities of Nb and Pd, Phys. Rev. B **23** (1981) 5080.

[43] J. P. Carbotte, Properties of boson-exchange superconductors, Rev. Mod. Phys. **62** (1990) 1027.

[44] S. Y. Savrasov and D. Y. Savrasov, Electron-phonon interaction and related physical properties of metals from linear-response theory, Phys. Rev. B **54** (1996) 16487.

[45] B. Mitrović, H. G. Zarate and J. P. Carbotte, The ratio $2\Delta_0/k_BT_c$ within Eliashberg theory, Phys. Rev. B **29** (1984) 184.

[46] X. H. Zheng and D. G. Walmsley, Extracting a more realistic pseudopotential for aluminium, lead, niobium and tantalum from superconductor electron tunnelling spectroscopy, J Low Temp. Phys. **166** (2012) 279.

[47] X. M. Chen and A. W. Overhauser, Effect of spin-density waves on the lattice dynamics of lead, Phys. Rev. B **39** (1989) 10570.

[48] A. W. Overhauser and T. M. Giebultowicz, Polarization of the spin-density waves in lead, Phys. Rev. B **57** (1993) 14338.

[49] R. Hooke and T. A. Jeeves, Direct search solution of numerical and statistical problems, J. Assoc. Comput. Math. **8** (1961) 212.

[50] X. H. Zheng and D. G. Walmsley, Evidence for effective weakening of electron-phonon interaction in superconducting tantalum, niobium, lead and aluminium, J. Low Temp. Phys. **173** (2013) 120.

[51] P. G. Tomlinson and J. P. Carbotte, Anisotropic superconducting energy gap in Pb, Phys. Rev. B **13** (1976) 4738.

[52] J. Nicol, S. Shapiro and P. H. Smith, Direct measurement of the superconducting energy gap, Phys. Rev. Lett. **5** (1960) 461.

[53] B. L. Blackford and R. H. March, Temperature dependence of the energy gap in superconducting Al-Al_2O_3-Al tunnel junctions, Can. J. Phys. **46** (1967) 141.

[54] C. Kittel, Introduction to solid state physics, John Wiley, New York, 1986, p 328.

[55] L. T. Claiborne and R. W. Morse, Study of the attenuation of ultrasonic shear waves in superconducting aluminium, Phys. Rev. **136**(1964) A893.

[56] M. A. Biondi, M. P. Garfunkel and W. A. Thompson, Millimeter-microwave studies of energy-gap anisotropy in superconductors, Phys. Rev. **136** (1964) A1471.

[57] Y. Kogure, N. Takeuchi, Y. Hiki, K. Mizuno and T. Kino, Anisotropy of energy gap in superconducting aluminium, J. de Phys. **46** (1965) C10-707.

[58] R. C. Dynes and J. P. Carbotte, Preferred direction tunnelling into a superconductor, Physica **55** (1971) 462.

[59] J. Bostock, K. Agyeman, M. H. Frommer and M. L. A. MacVicar, Determining accurate superconducting tunnelling energy gap, J Appl. Phys. **44** (1973) 5567.

[60] M. L. A. MacVicar and R. M. Rose, Anisotropic energy-gap measurements on superconducting niobium single crystals by tunnelling, J. Appl. Phys. **39** (1968) 1721.

[61] M. L. A. MacVicar, Distribution of the energy gap in k space for superconducting Nb, Phys. Rev. B **2** (1970) 97.

[62] E. L. Wolf, J. Zasadzinski, J. W. Osmun and G. B. Arnold, Proximity electron tunnelling spectroscopy I. experiments on Nb, J Low Temp Phys **40** (1980) 19.

[63] R. Dobbs and M. Perz, Anisotropy of the energy gap in niobium from ultrasonic measurements, Rev. Mod. Phys. **36** (1964) 257.

[64] A. Hahn, S. Hofmann, A Krause and P. Seidel, Tunnelling results on gap anisotropy in niobium, Physica C **296** (1998) 103.

[65] J. Daams and J. P. Carbotte, Thermodynamic properties of superconducting niobium, J. Low Temp. Phys. **40** (1980) 135.

[66] S. M. Durbin, D. S. Buchanan, J. E. Cunningham and D. M. Ginsberg, Observation of tunnelling anisotropy in superconducting niobium crystals, Phys. Rev. B **28** (1983) 6277.

[67] Z. W. Sarafi, Ultrasonic attenuation in superconducting tantalum, NASA Tech. Note **TN D-4806** (1968) 1.

[68] H. J. Choi, D. Roundy, H. Sun, M. L. Cohen and S. Louie, The origin of the anomalous superconducting properties of MgB_2, Nature **418** (2002) 758.

[69] M. P. Allan, F. Massee, D. K. Morr, J, Van Dyke, A. W. Rost, A. P. Mackenizie, C. Petrovic and J. C. Davis, Imaging Cooper pairing of heavy fermions in $CeCoIn_5$, Nature Phys. **9** (2013) 468.

[70] B. B. Zhou, S. Misra, E. H. da Silva Neyo, P. Aynajian, R. E. Baumbach, J. D. Thompson, E. D. Bauer and A. Yazdani, Visualizing nodal heavy fermion superconductivity in $CeCoIn_5$, Nature Phys. **9** (2013) 474.